Radiotherapy and Oncology 207 (2025) 110879

Contents lists available at ScienceDirect

Radiotherapy and Oncology

journal homepage: www.thegreenjournal.com

Original Article

Integration test of biaxially rotational dynamic-radiation therapy for nasopharyngeal carcinoma: Efficacy evaluation and dosimetric analysis

Shinya Hiraoka [a], Hideaki Hirashima [a], Mitsuhiro Nakamura [b], Fumiya Tanaka [c], Hiroki Adachi [c], Yuka Ono [a], Tomohiro Ono [a,d], Ryota Nakashima [a], Aya Nakajima [a], Takashi Mizowaki [a,*]

[a] Department of Radiation Oncology and Image-Applied Therapy, Graduate School of Medicine, Kyoto University, Japan
[b] Department of Advanced Medical Physics, Graduate School of Medicine, Kyoto University, Japan
[c] X-ray Therapy Division, Therapy System Business, Healthcare Business Group, Hitachi High-Tech Corporation, Tokyo, Japan
[d] Department of Radiation Oncology, Shiga General Hospital, Shiga, Japan

ARTICLE INFO

Keywords:
Non-coplanar VMAT
Coplanar VMAT
Head and neck
Nasopharyngeal carcinoma
BROAD-RT

ABSTRACT

Background and Purpose: OXRAY is a new O-ring-shaped radiotherapy system delivering biaxially rotational dynamic-radiation therapy (BROAD-RT), a technique that enables non-coplanar volumetric-modulated arc therapy (VMAT) for large target volumes without requiring couch movement. The purpose of this study was to evaluate the benefits of BROAD-RT and to perform an integration test to confirm the plan deliverability and its accuracy from the treatment planning system to OXRAY for patients with nasopharyngeal carcinoma.

Methods and Materials: We compared treatment plans for BROAD-RT and coplanar VMAT (COVMAT) created in RayStation for 15 patients with nasopharyngeal cancer using the Wilcoxon signed-rank test. *P* values less than 0.05 were considered statistically significant. Additionally, we confirmed the plan delivery accuracy of BROAD-RT from the treatment planning system to OXRAY; gamma passing rates (GPRs) and delivery time were evaluated. The criteria for pass and fail were ≥95 % at γ3%2 mm.

Results: BROAD-RT significantly improved the homogeneity and conformity index of planning target volume and reduced dose volume indices compared with COVMAT in $D_{0.03\ cc}$ for the brainstem, $D_{0.03\ cc}$ for the left optic nerve, $D_{0.03\ cc}$ for the brachial plexus, D_{mean} for each submandibular gland, D_{mean} for the oral cavity, and D_{mean} for each parotid gland. All plans for BROAD-RT passed the integration test; the mean GPR (3 %/2 mm) was above 95 % and the median delivery time was 209 s.

Conclusions: BROAD-RT delivered by OXRAY passed the integration test, and it demonstrated the potential benefit of improving the dose distribution compared with COVMAT for patients with nasopharyngeal carcinoma.

Introduction

Nasopharyngeal carcinoma is a rare disease, accounting for 0.7 % of all cancers worldwide; its geographical distribution is unequal, with 70 % of cases occurring in East and Southeast Asia [1]. Radiotherapy for nasopharyngeal carcinoma is the standard treatment not only for early stage to locally advanced disease but also for selected cases of metastatic disease [2,3], which requires large irradiation fields ranging from the skull base to the superior mediastinum [4]. Importantly, the head and neck region contain many vital organs related to quality-of-life functions such as communication, nutrition, and respiration. However, the large radiation fields for the head and neck region cause great damage to vital organs, leading to adverse side effects [5].

Compared to three-dimensional conformal radiotherapy (3D-CRT), intensity-modulated radiation therapy (IMRT) and coplanar volumetric-modulated arc therapy (COVMAT) can improve the dose coverage for

Abbreviations: IMRT, intensity-modulated radiation therapy; COVMAT, coplanar volumetric-modulated arc therapy; 3D-CRT, three-dimensional conformal radiotherapy; BROAD-RT, biaxially rotational dynamic-radiation therapy; DWA, Dynamic WaveArc®; OAR, organ at risk; GTV, gross tumor volume; CTV, clinical target volume; PTV, planning target volume; DVIs, dose-volume indices; HI, homogeneity index; CI, Paddick conformity index; MUs, monitor units.

* Corresponding author at: Department of Radiation Oncology and Image-Applied Therapy, Graduate School of Medicine, Kyoto University, 54 Shogoin Kawahara-cho, Sakyo-ku, Kyoto 606-8507, Japan.
E-mail address: mizo@kuhp.kyoto-u.ac.jp (T. Mizowaki).

https://doi.org/10.1016/j.radonc.2025.110879
Received 16 October 2024; Received in revised form 27 March 2025; Accepted 30 March 2025
Available online 4 April 2025

tumor volume by decreasing the dose to adjacent organs. This approach has improved tumor control for patients with head and neck cancer [6]. Despite recent advancements in radiotherapy, many patients continue to experience severe adverse effects, highlighting the need for further enhancements in radiotherapy techniques [7]. In recent years, non-coplanar VMAT techniques that effectively reduce low- and intermediate-radiation doses have garnered increasing attention [8]. However, non-coplanar VMAT is not commonly used for head and neck cancer because it is time consuming and has the potential risk of collision with the patient [9–13].

In 2008, Mitsubishi Heavy Industries, Ltd., Japan, introduced the Vero4DRT system, an advanced image-guided radiation therapy system featuring unique capabilities for clinical use [14]. A distinctive feature is the biaxially rotational dynamic-radiation therapy (BROAD-RT), also known as three-dimensional unicursal irradiation [15]. This technique enables non-coplanar VMAT by simultaneous gantry and O-ring rotation without patient couch movement. This approach is also referred to as Dynamic WaveArc® (DWA), a part of BROAD-RT, and it is known to enhance dose distribution across various treatment sites [16–19]. However, the DWA in Vero4DRT possesses three critical limitations: limited radiation field size [20,21], which makes it unsuitable for treating large tumors; lack of gimbal operation support during VMAT [22]; and user-dependent customization of DWA trajectories constrained by mechanical limitations. Vero4DRT encountered some challenges in interfacing with the treatment planning system, which resulted in significant delays in its development [23].

In June 2023, Hitachi Ltd. released its second-generation O-ring-shaped image-guided therapy system, OXRAY [24]. With improved mechanical performance and a close collaboration with RaySearch Laboratories AB, OXRAY was able to integrate BROAD-RT (Dynamic SwingArc®) with the gimbal head rotation, leading to extended-field non-coplanar radiotherapy with customizable trajectories. These improvements have addressed the critical limitations in Vero4DRT.

We report on a comparison of an integration test using this novel BROAD-RT with gimbal planning approach for 15 nasopharyngeal carcinoma case datasets to quantify the potential benefit of BROAD-RT with gimbal using customizable trajectories and enlarge the radiation fields with gimbal swinging up to 3° without couch movement to reduce the organ-at-risk (OAR) dose compared to that in COVMAT. The delivery accuracy was evaluated by irradiation verification in phantom experiments.

Methods and Materials

System overview of OXRAY

OXRAY utilizes a sturdy O-ring-shaped structure and gimbaled head with an ultracompact C-band linear accelerator. A brief comparison of the specifications of Vero4DRT, OXRAY, and TrueBeam is shown in Table 1. The gantry rotates within the ring at a maximum speed of 7°/s, allowing ± 185° rotation. Additionally, the O-ring rotates around its vertical axis with a maximum speed of 6°/s within a range of ± 60°. The gantry and ring can rotate independently while the treatment couch is fixed. OXRAY offers X-ray energies of 6 MV and 6 MV-flattening filter free (FFF), with maximum dose rates of 600 MU/min and 1200 MU/min, respectively. The image guidance system includes a dual kilovoltage X-ray imaging system, able to perform a fast dual-source cone-beam computed tomography requiring only 15 s of scanning time. Moreover, a robotic treatment couch is available to correct the patient position with five degrees of freedom (three axes of translation and two axes of rotation).

The gimbaled head can rotate with two orthogonal gimbals, independently allowing pan and tilt rotations of up to ± 3°. The maximum rotational speed is 6°/s. With this rotational capability, the beam swing can reach up to ± 50.3 mm in each direction on the isocenter plane. This enables an irradiation coverage area up to 30 × 30 cm, although the

Table 1
Comparison of specifications among Vero4DRT, OXRAY, and TrueBeam.

	Vero4DRT	OXRAY	TrueBeam
Mechanical characteristics			
Gantry rotational speed	7°/s	7°/s	6°/s
O-ring rotational speed	3°/s	6°/s	N/A
Gantry stroke	±185°	±185°	±185°
O-ring stroke	±60°	±60°	N/A
Table stroke	N/A	N/A	±100°
Irradiation system			
Gimbal stroke	±2.5°	±3.0°	N/A
Beam energy (dose rate)	6 MV (500 MU/min)	6 MV (600 MU/min) and 6 MV-FFF (1200 MU/min)	4 MV (250 MU/min), 6 MV (600 MU/min), 8 MV (600 MU/min), 10 MV (600 MU/min), 15 MV (600 MU/min), 6 MV-FFF (1400 MU/min), and 10 MV-FFF (2400 MU/min)
Maximum field size	15 × 15 cm	20 × 20 cm (without gimbal rotation) 30 × 30 cm (with gimbal rotation)	40 × 40 cm
MLC leaf width	5 mm (30 pairs)	2.5 mm (16 pairs: ±40 mm of the isocenter) 5 mm (32 pairs: other)	5 mm (40 pairs: ±200 mm of the isocenter) 10 mm (20 pairs: other)
MLC speed@iso	50 mm/s	65 mm/s	25 mm/s
Imaging system			
Orthogonal kV X-ray imaging device (FPD)			
SAD	100 cm	105.97 cm	100 cm (variable)
Pixels	1,024 × 768 (2 × 2 binning)	1,440 × 1,440 (2 × 2 binning)	1,024 × 768
Bit depth	14	16	16
Resolution@iso	0.21 mm	0.15 mm	0.38 mm
Pixel area@iso	21 × 16 cm	21 × 21 cm	39.7 × 29.8 cm
CBCT FOV	21 (diameter) × 16 cm	21 (diameter) × 21 cm40 (diameter) × 21 cm (FPD position shift)	24 (diameter) × 18 cm (full fan mode) 45 (diameter) × 16 cm (half fan mode: FPD position shift)
MV X-ray imaging device (EPID)			
Pixels	1,024 × 1,024 (2 × 2 binning)	1,536 × 1,536 (2 × 2 binning)	1,280 × 1,280
Bit depth	16	16	16
Resolution@iso	0.18 mm	0.13 mm	0.33 mm
Pixel area@iso	18 × 18 mm	19.8 × 19.8 cm	43 × 43 cm
Positioning system			
Positioning function	ExacTrac	Hitachi PIAS technology	kV X-ray imaging
IR camera		Integration	
Robotics		5-axis + O-ring rotation	

Abbreviations: MLC, multi-leaf collimator; FPD, flat panel detector; SAD, source-axis distance; iso, isocenter; CBCT, cone beam computed tomography; FOV, field of view; EPID, electronic portal imaging device; IR, infrared; N/A, not available; FFF, flattening filter free; MU, monitor unit.

maximum field size of the multi-leaf collimator (MLC) is 20 × 20 cm.

Overview of the integration test

OXRAY is a new radiotherapy system, and its robustness has not been evaluated so far. Thus, we conducted an integration test according to actual clinical flow. First, we created test plans on a treatment planning system (RayStation version 2023B; RaySearch Laboratories, Stockholm, Sweden) using actual clinical data. Next, we transferred the plans from RayStation to OXRAY and confirmed that OXRAY could translate the plans into operation. Finally, through geometric and dosimetric assessments, we confirmed that OXRAY could successfully deliver the planned doses with required accuracy.

Patient data

We enrolled 15 nasopharyngeal carcinoma patients who had undergone definitive radiotherapy at our institution between 2015 and 2021. Patients were immobilized in a supine position by a thermoplastic mask (Uni-frame Thermoplastics; CQ Medical, Avondale, PA, USA). CT images were acquired using a 512 × 512 matrix with ≤ 2.5 mm slice thickness (voxel size, 0.97 × 0.97 × 2.5 mm) on the LightSpeed RT platform (GE Healthcare, Little Chalfont, UK) and SOMATOM Definition (Siemens Medical Systems, Erlangen, Germany). The study protocol was approved by our Institutional Review Board (R1048).

Patient characteristics

The median age was 58 years (range, 30–84), and 11 patients (73.3 %) were male. The clinical stage was II in six (40.0 %), III in six (40.0 %), and IVA in three patients (20 %) according to the criteria of the Union for International Cancer Control 8th edition [25].

Contouring targets and organs at risk

The gross tumor volume of primary tumor (GTVp) and that of lymph node metastases (GTVn) were delineated with reference to CT and magnetic resonance imaging (MRI) data and the findings of fluorodeoxyglucose-positron emission tomography (FDG-PET); fiber-optic endoscopic findings were also referred to the GTV. MRI and FDG-PET were fused to CT using rigid image registration. GTV was defined as GTVp plus GTVn. The high-risk clinical target volume (CTV) was the GTV area plus a margin of 5 mm and the whole nasopharyngeal mucosa. The intermediate-risk CTV included the GTV area plus a margin of 10 mm, high-risk lymph node area, and adjacent structures of the nasopharynx. Low-risk CTV included the low-risk lymph node area. Planning target volume (PTV) was defined as each CTV plus a 5-mm setup margin trimmed to 3 mm under the skin [4]. Brainstem, spinal cord, cochlea, submandibular gland, parotid gland, oral cavity, optic nerve, temporal lobe, lens, eyeballs, brachial plexus, hippocampi, and larynx were delineated as the OARs [26]. Organs located on both sides of the body, except for the lens, eyeballs, brachial plexus, and hippocampus, were delineated separately. Planning OAR volume (PRV) margins on the brainstem, spinal cord, and optic nerve were 3 mm. All critical structures, such as OARs, were first manually contoured by medical physicists, and radiation oncologists then assessed and revised the structures for accuracy. Target volumes were contoured by expert radiation oncologists.

Treatment planning

COVMAT and BROAD-RT plans were generated in a research version of RayStation version 2023B. The dose calculation algorithm in all treatment plans was collapsed cone in RayStation, and the grid size was set to 2 mm. Because of the limitation of the maximum field size, OXRAY cannot cover the entire PTV with COVMAT for patients with nasopharyngeal carcinoma. Additionally, the extended irradiation field associated with gimbal rotation enables irradiation from more non-coplanar angles. Thus, COVMAT plans were created for the 6-MV flattened photon beam generated by TrueBeam (Varian Medical Systems, Washington DC, USA) using a two-full-rotation coplanar arc trajectory. In addition, BROAD-RT plans were created for a 6-MV flattened photon beam generated by OXRAY using two non-coplanar dynamic trajectories with a gimbal rotation of ± 2° in the tilt direction, to extend the irradiation range in the cranio-caudal direction; the value was set in RayStation manually (Supplementary Fig. 1). Fig. 1 shows the arc trajectories of BROAD-RT and COVMAT. To avoid multiple comparisons, we selected the representative trajectory in BROAD-RT using the following methodology. First, a template trajectory in OXRAY, which can avoid shoulder irradiation, was selected. We developed a collision map software available for OXRAY to evaluate the risk of collision at any ring and gantry angle, which is not implemented in RayStation [18]. To improve the flexibility of optimization, the ring angle was set to the maximum value by referring to the collision map. In addition, the trajectories were simplified to shorten the delivery time (Supplementary Fig. 2) [27]. We defined manipulation points as gantry and ring angle positions where the direction of O-ring rotation can be changed. Manipulation points of the trajectories used in this study are shown in Supplementary Table 1.

The prescribed dose of 70 Gy in 35 fractions was administered to 95 % of the high-risk PTV (PTV70 $D_{95\%}$) for each plan. The simultaneous integrated boost technique was used to deliver 70 Gy, 63 Gy, and 56 Gy for PTV70, intermediate-risk PTV (PTV63), and low-risk PTV (PTV56), respectively, in 35 fractions. Dose constraints and priority of planning are listed in Table 2. PRV dose constraints were not set; however, PRV was used for optimization structures.

To minimize planning bias and ensure consistency, we developed a script that automatically applied the same optimization conditions as a template and performed three rounds of automatic optimization for each plan. Specifically, this script inserted a standardized set of optimization parameters for all plans and automatically ran three consecutive optimization cycles. After this automated process, if any dose constraints were not met, we made a single manual adjustment by modifying the weight of the relevant ROI. This approach allowed us to maintain a high degree of consistency across all plans while minimizing manual intervention. After target delineation, planning optimization was performed by the radiation oncologist, and the quality and acceptability of the plan were evaluated together by the radiation oncologist and medical physicist.

Plan evaluation

Dose-volume indices (DVIs) for $D_{2\%}$, $D_{10\%}$, $D_{50\%}$, $D_{90\%}$, and $D_{98\%}$ of PTV and $D_{98\%}$ of GTVp were evaluated. In addition, DVIs for OAR, such as $D_{0.03\ cc}$ for the brainstem, spinal cord, optic nerve, lens, eyeball, and temporal lobe, and D_{mean} for submandibular gland, oral cavity, parotid gland, cochlea, hippocampi, and larynx were assessed. Homogeneity index (HI), defined as $(D_{2\%} - D_{98\%})/D_{50\%}$, was calculated for each PTV [28]. Paddick conformity index (CI), defined as $(V_{PTV,\ ref})^2/(V_{PTV} \times V_{ref})$, was calculated for each PTV. $V_{PTV,\ ref}$ is the PTV volume within the prescribed dose, V_{PTV} is the PTV volume, and V_{ref} is the volume in the body [29]. The CI of PTV63 and PTV56 is underestimated because doses of 63 Gy and 56 Gy or more are delivered to PTV70 and PTV70 + PTV63, respectively. Therefore, V_{ref} values of 63 Gy and 56 Gy were excluded from PTV70 and PTV70 + PTV63, respectively. Our study was given a rating score according to the RATING guidelines, which provides a quality framework of recommendations and contributes to the quality of planning studies and the resulting publications [30].

In addition, to assess plan complexity, we evaluated two complexity indices, modulation complexity score for VMAT (MCSv) and aperture area variability (AAV), in both COVMAT and BROAD-RT [31,32]. The calculated monitor units (MUs), planning time from optimization to

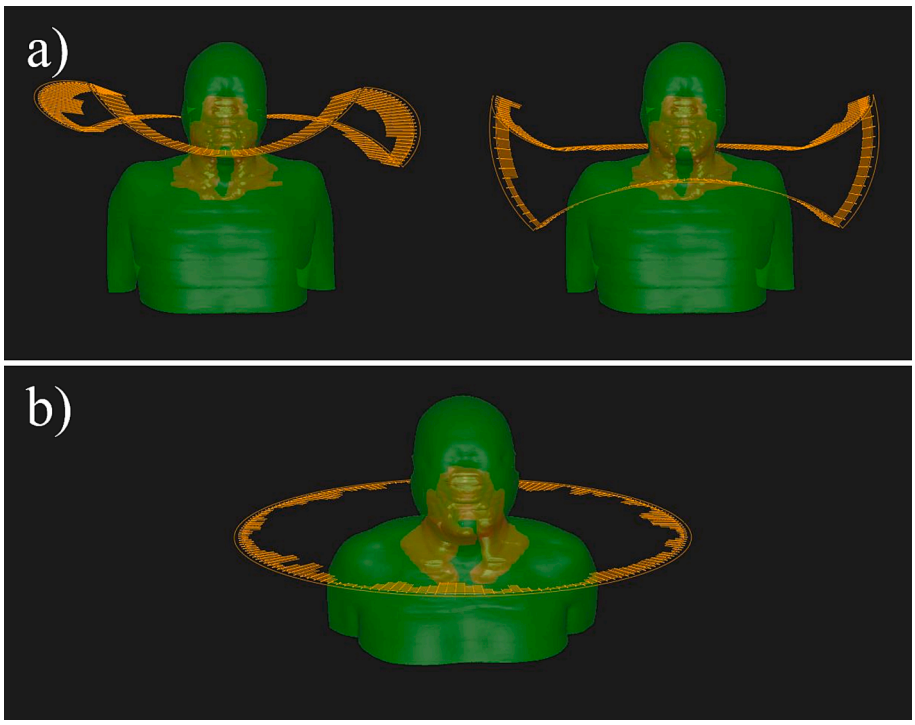

Fig. 1. (a) Arc trajectories of BROAD-RT; both trajectories were modified to avoid shoulder irradiation. Additionally, the trajectories of RING angle were modified with reference to a collision map. The angle of gimbal tilt rotation was −2° for the arc on the left side and +2° for the arc on the right side. (b) Arc trajectories of coplanar VMAT. Abbreviations: BROAD-RT, biaxially rotational dynamic-radiation therapy.

Table 2
Dose constraints and priority of planning.

Structure	Index	Dose constraints		Priority
		Hard	Soft	
Body	D_{max}	<77 Gy	<80 Gy	High
PTV70	$D_{95\%}$	70 Gy		High
PTV63	$D_{50\%}$	63 Gy	61.0–64.9 Gy	High
PTV56	$D_{50\%}$	56 Gy	54.0–57.7 Gy	High
GTV	$D_{98\%}$	>73 Gy	>70 Gy	High
Spinal cord	D_{max}	< 40 Gy	< 46 Gy	High
Brainstem	D_{max}	<54 Gy	<63 Gy	High
Brachial plexus	D_{max}	<66 Gy	<70 Gy	Moderate
Optic nerve	D_{max}	<55 Gy	<60 Gy	Moderate
Temporal lobe	D_{max}	<63 Gy	<74 Gy	Moderate
Lens	D_{max}	<6 Gy	<10 Gy	Moderate
Eyeballs	D_{max}	<35 Gy	<45 Gy	Moderate
Submandibular gland	D_{mean}	<39 Gy	<50 Gy	Low
Parotid gland	D_{mean}	<26 Gy	<30 Gy	Moderate
Oral cavity	D_{mean}	<45 Gy	<50 Gy	Moderate
Larynx	D_{mean}	<30 Gy	<45 Gy	Low
Cochlea	D_{mean}	<45 Gy	<50Gy	Moderate

Abbreviations: PTV, planning target volume; GTV, gross tumor volume; D_{max}, max dose to structure; $D_{x\%}$, minimal dose to most exposed x% of structure; D_{mean}, mean dose to structure.

completion of dose distribution calculation, and delivery time were also recorded.

Geometric and dosimetric accuracy

To assess the geometric accuracy of BROAD-RT, two types of log files were collected: the MLC log file and the control log file. These files recorded both planned and actual values for the MLC position, gantry angle, O-ring angle, gimbal pan angle, gimbal tilt angle, and MU at 20-ms intervals. The mean absolute error (MAE) was calculated for each parameter.

To assess the dosimetric accuracy, the calculated and measured dose distributions of BROAD-RT were assessed according to global gamma analysis using ArcCHECK (Sun Nuclear, Melbourne, FL, USA) (Supplementary Fig. 3). The criteria of gamma passing rate (GPR) were 3 % of the planned maximum dose as the dose-difference criterion and 2 mm as the distance-to-agreement criterion, with a 10 % threshold; the criteria for pass and fail were ≥ 95 % at γ3%2mm according to AAPM-TG218 [33].

Statistical analysis

DVIs, HI, CI, MCSv, and AAV for BROAD-RT and COVMAT were compared using the Wilcoxon signed-rank test. *P* values less than 0.05 were considered statistically significant. All statistical analyses were conducted with R (version 4.3.1, the R Foundation for Statistical Computing, Vienna, Austria).

Results

The median PTV volume (PTV70 + PTV63 + PTV56) was 995.6 cm^3 (range, 678.6–1201.0). The representative dose distributions are shown in Fig. 2. A comparison of HI and DVIs is shown in Table 3. Dose-volume histograms are shown in Fig. 3. BROAD-RT significantly improved HI of PTV70/63/56 and CI of PTV70/56 compared with COVMAT. Additionally, BROAD-RT enabled a significant dose reduction compared with COVMAT in $D_{0.03\ cc}$ for the brainstem, $D_{0.03\ cc}$ for the left optic nerve, $D_{0.03\ cc}$ for the brachial plexus, D_{mean} for the left submandibular gland, D_{mean} for the right submandibular gland, D_{mean} for the oral cavity, D_{mean} for the left parotid gland, and D_{mean} for the right parotid gland. No significant difference was found in $D_{0.03\ cc}$ (spinal cord, right optic nerve, temporal lobe, eyeballs, and lens) and D_{mean} (left cochlea, right cochlea, hippocampi, and larynx). No OARs achieved significant dose reduction by COVMAT compared with BROAD-RT.

The mean ± standard deviations (SDs) of MCS and AAV were 0.21 ± 0.03 and 0.13 ± 0.02, respectively, for COVMAT, and 0.11 ± 0.01 and

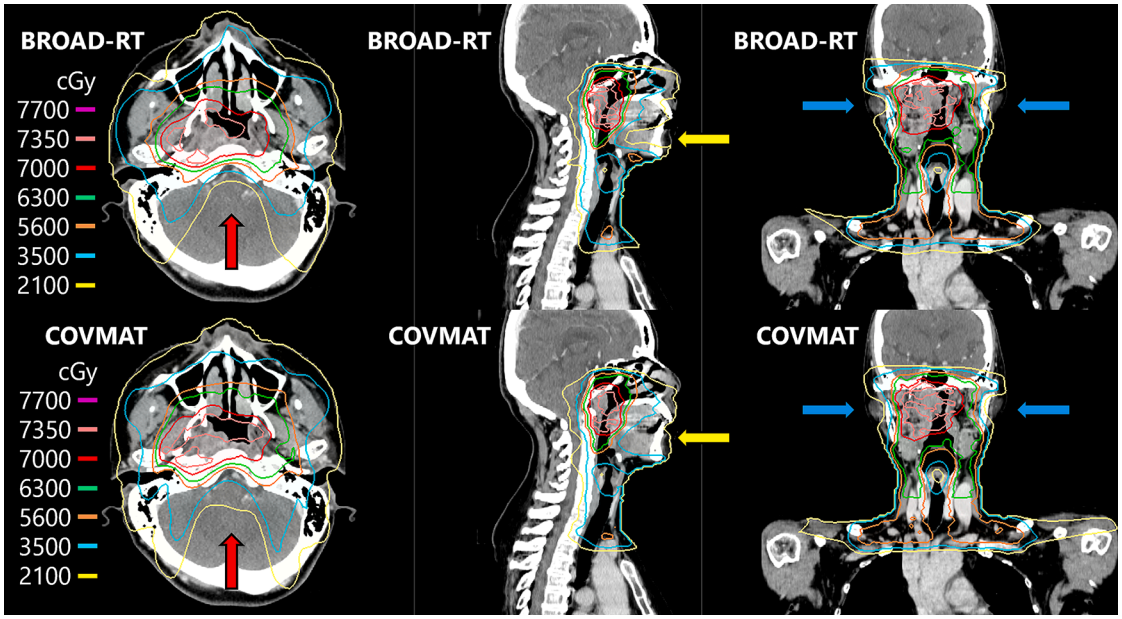

Fig. 2. Representative dose distributions of BROAD-RT and COVMAT (axial, sagittal, and coronal views). Red arrows indicate that BROAD-RT reduced brainstem dose compared with COVMAT. Yellow arrows indicate that BROAD-RT reduced oral cavity dose compared with COVMAT. Blue line indicates that BROAD-RT provided a steeper dose gradient around deep parotid glands, resulting in a dose reduction of parotid glands compared with COVMAT. Abbreviations: BROAD-RT, biaxially rotational dynamic-radiation therapy; COVMAT, coplanar VMAT.

0.11 ± 0.02, respectively, for BROAD-RT. The differences between the two techniques were statistically significant ($p < 0.05$).

The median value of MUs and delivery time for BROAD-RT (range: min–max) were 1296 MU (1185–1478) and 209 s (192–247), respectively, and those for COVMAT were 807 MU (722–1008) and 146 s (139–157), respectively. The median value of planning time from optimization to completion of dose distribution calculation for BROAD-RT and COVMAT was 212 s (192–247) and 146 s (139–157), respectively. The overall RATING score was 98 % (supplementary Table 2).

The MAE for the gantry angle, O-ring angle, pan angle, tilt angle, MLC position, and MU during BROAD-RT was 0.10°, 0.06°, 0.02°, 0.06°, 0.05 mm, and 0.3 MU, respectively. All plans of BROAD-RT passed the integration test, and the mean ± SD of GPR (3 %/2 mm) was 98.4 ± 0.9 %.

Discussion

We conducted the integration test to evaluate the efficacy of BROAD-RT and confirm the plan deliverability and its accuracy from the treatment planning system to OXRAY for patients with nasopharyngeal carcinoma. BROAD-RT significantly improved the dose distribution compared with COVMAT, without couch movement. Furthermore, the BROAD-RT plans passed the integration test, and the delivery accuracy and delivery time of BROAD-RT were clinically acceptable.

A typical non-coplanar VMAT technique that can be delivered on a conventional C-arc linac uses a fixed-angle couch; however, beam directions are limited because of the fixed-angle couch position [11,12,34]. In this regard, a trajectory VMAT technique that combines dynamic couch rotation with dynamic gantry rotation (non-coplanar dynamic trajectory VMAT) potentially overcomes the limited beam directions without collision and can provide beam directions with high flexibility. Fix et al. reported the concept of non-coplanar dynamic trajectory VMAT for head and neck cancers [13]. Bertholet et al. reported that non-coplanar dynamic trajectory VMAT for head and neck cancers is deliverable on C-arm linac with high dosimetric accuracy [9,35]. However, non-coplanar dynamic trajectory VMAT was not yet clinically available because of factors such as long delivery time, complicated movement of the treatment couch, and working only in developer mode. In contrast, OXRAY has already been clinically implemented, enabling the application of BROAD-RT in the treatment of patients with head and neck cancers. Notably, BROAD-RT operates without requiring couch movement, enabling a higher ring rotation speed compared to the table rotation speed of C-arm platforms (6°/s vs. 3°/s). Compared to non-coplanar dynamic trajectory VMAT, these features contribute to shorter treatment durations and a reduction in couch positioning errors induced during the treatment process [36]. This study is the first to report the potential application of BROAD-RT for nasopharyngeal carcinoma based on direct comparison of key dosimetric parameters and delivery times of the BROAD-RT and COVMAT plans.

BROAD-RT significantly improved the dose distribution compared with COVMAT, without couch movement. Leitao et al. generated whole-neck plans for 20 nasopharyngeal carcinoma patients using COVMAT or the typical non-coplanar VMAT technique. Their results indicated that the typical non-coplanar VMAT significantly reduced the dose to OARs with similar target coverage compared with COVMAT (mean dose reduction of the left parotid, right parotid, left submandibular gland, and oral cavity by 3.9 Gy, 2.2 Gy, 3.8 Gy, and 2.6 Gy, respectively) [11]. Subra et al. developed whole-neck plans for 22 patients with head and neck cancers; they also indicated that typical non-coplanar VMAT significantly reduced the dose to OARs with similar target coverage compared with COVMAT (mean dose reduction of the parotid glands, larynx, and oral cavity by 3 Gy, 4 Gy, 5 Gy, and 4.3 Gy, respectively) [37]. These reports support our results that BROAD-RT significantly reduced the dose to OARs compared with COVMAT. Although the typical non-coplanar VMAT for head and neck cancers could not achieve improvement in PTV homogeneity in previous studies [11,37], BROAD-RT resulted in a significant improvement compared with COVMAT. Notably, this advantage might be attributed to the higher flexibility of the beam directions in BROAD-RT, although it is not a direct comparison between BROAD-RT and the typical non-coplanar VMAT [13,35].

The non-coplanar VMAT for head and neck cancers has been reported to be time consuming, limiting its integration in clinical practice [8]. Bertholet et al. reported that the delivery time of whole-neck irradiation for locoregionally advanced oropharyngeal carcinoma using non-coplanar dynamic trajectory VMAT with one or two full arcs was 10.4 min [35]. Gayen et al. also reported that the mean delivery time of

Table 3
Comparison of homogeneity index, conformity index, and dose-volumetric indices between BROAD-RT and COVMAT.

		BROAD-RT		COVMAT		*p*-value
		Mean	SD	Mean	SD	
PTV70	HI	0.12	0.03	0.15	0.04	**<0.001**
	CI	0.82	0.06	0.76	0.10	**0.01**
	$D_{98\%}$ (Gy)	67.98	1.02	67.55	1.09	**0.005**
	$D_{95\%}$ (Gy)	70.03	0.02	70.00	0.00	**0.002**
	$D_{90\%}$ (Gy)	71.35	0.42	71.66	0.61	**0.002**
	$D_{50\%}$ (Gy)	74.26	1.12	75.13	1.40	**0.001**
	$D_{10\%}$ (Gy)	75.78	1.53	77.38	1.92	**<0.001**
	$D_{2\%}$ (Gy)	76.72	1.84	78.90	2.39	**<0.001**
PTV63	HI	0.27	0.03	0.31	0.05	**0.002**
	CI	0.67	0.08	0.65	0.08	0.14
	$D_{98\%}$ (Gy)	54.15	1.96	53.16	2.03	0.41
	$D_{95\%}$ (Gy)	58.16	1.57	57.31	1.60	0.21
	$D_{90\%}$ (Gy)	60.79	1.41	60.21	1.23	0.23
	$D_{50\%}$ (Gy)	65.68	1.19	66.29	1.30	**0.002**
	$D_{10\%}$ (Gy)	68.98	1.33	70.66	1.91	**<0.001**
	$D_{2\%}$ (Gy)	71.72	1.23	73.58	2.09	**<0.001**
PTV56	HI	0.09	0.02	0.12	0.03	**<0.001**
	CI	0.38	0.10	0.31	0.09	**<0.001**
	$D_{98\%}$ (Gy)	55.44	1.39	54.47	1.58	**<0.001**
	$D_{95\%}$ (Gy)	56.61	1.18	55.98	1.26	**0.004**
	$D_{90\%}$ (Gy)	57.31	1.06	56.98	1.16	0.06
	$D_{50\%}$ (Gy)	58.49	1.07	59.01	1.22	**0.005**
	$D_{10\%}$ (Gy)	59.41	1.22	60.48	1.45	**<0.001**
	$D_{2\%}$ (Gy)	60.56	1.56	61.83	1.81	**<0.001**
GTVp $D_{98\%}$ (Gy)		72.74	1.00	72.43	0.99	0.36
Left parotid gland Dmean (Gy)		28.91	7.30	29.78	7.00	**0.02**
Right parotid gland Dmean (Gy)		27.03	5.91	27.79	5.83	**0.03**
Oral cavity Dmean (Gy)		35.79	6.76	40.10	6.69	**<0.001**
Larynx Dmean (Gy)		30.62	6.25	30.46	7.67	>0.99
Brain Stem $D_{0.03\ cc}$ (Gy)		40.94	10.65	48.38	7.09	**<0.001**
Spinal Cord $D_{0.03\ cc}$ (Gy)		36.46	3.21	37.51	4.03	0.15
Left cochlea Dmean (Gy)		39.26	16.54	40.71	16.99	0.21
Right cochlea Dmean (Gy)		33.65	9.26	35.64	10.50	0.33
Left Glnd_Submand Dmean (Gy)		63.17	9.03	64.90	8.50	**<0.001**
Right Glnd_Submand Dmean (Gy)		66.12	5.18	67.39	5.89	**0.004**
Left optic nerve $D_{0.03\ cc}$ (Gy)		24.88	21.51	28.39	19.96	**0.03**
Right optic nerve $D_{0.03\ cc}$ (Gy)		30.97	18.07	38.85	17.14	0.17
Temporal lobe $D_{0.03\ cc}$ (Gy)		72.46	4.27	72.85	5.34	0.50
Hippocampi Dmean (Gy)		6.60	4.21	6.11	2.97	0.93
Brachial plexus $D_{0.03\ cc}$ (Gy)		65.20	5.59	66.21	5.55	**0.04**
Eyeballs $D_{0.03\ cc}$ (Gy)		23.17	7.18	20.40	9.03	0.08
Lens $D_{0.03\ cc}$ (Gy)		5.72	3.53	4.40	1.44	0.14

Abbreviations: PTV, planning target volume; BROAD-RT, biaxially rotational dynamic radiation therapy; COVMAT, coplanar volumetric modulation arc therapy; HI, homogeneity index; CI, Paddick conformity index; SD, standard deviation; Glnd_Submand, submandibular gland.
Note: The *p*-values in bold indicate statistical significance.

whole-neck irradiation for head and neck cancers using the typical non-coplanar VMAT with two partial arcs was 12.0 min [12]. Previous studies reported that the use of highly complex non-coplanar arcs, incorporating gantry, table, and collimator rotations, resulted in prolonged beam delivery times. In contrast, our results demonstrate that the median delivery time for BROAD-RT using two arcs was only 3.5 min. Although a direct comparison between BROAD-RT and the typical non-coplanar dynamic trajectory VMAT was not performed, these findings suggest that BROAD-RT may achieve the shortest delivery time for whole-neck irradiation among the non-coplanar VMAT techniques. Additionally, the short delivery time of OXRAY may help ensure the accuracy of radiotherapy because the delivery time correlates with the intra-fractional errors [36]. Furthermore, couch movement is not required with BROAD-RT, because of which OXRAY can minimize intra-fractional error by image guidance before treatment. However, non-coplanar dynamic trajectory VMAT using C-arm linac requires couch movement, because of which it is necessary to consider intra-fractional error caused by not only the accuracy of couch movement but also the movement of the patient. Considering the advantage of BROAD-RT, which does not involve couch movement, BROAD-RT may be considered the most practical irradiation technique compared with previously reported techniques of non-coplanar VMAT.

The dose per fraction of radiotherapy for head and neck cancers is generally low [2]. Therefore, it is difficult to make the most use of the high dose rate of the FFF beam. Thus, using a 6-MV flattened filter beam has been considered sufficient for research in head and neck cancers [9,13,35]. We expect a potential benefit of using a 6-MV FFF beam for head and neck cancers in terms of beam-on-time efficiency, and further research is needed.

Verifying the accuracy of the new beam delivery techniques is essential. BROAD-RT exhibits a high level of complexity because of the independent rotation of the gantry and ring. Our analysis showed that BROAD-RT achieved significantly lower MCSv and AAV metric values compared to COVMAT. This result is likely attributable to the increased plan complexity of BROAD-RT, which utilizes a non-coplanar arc, resulting in a higher MU value than that observed with COVMAT [8].

Further investigations into the geometric and dosimetric accuracy of BROAD-RT were conducted. The delivery accuracy of BROAD-RT met the clinically acceptable criteria defined by the American Association of Physicists in Medicine Task Group 218 [33]. Moreover, the geometric and dosimetric accuracy of BROAD-RT was found to be equivalent to that of DWA, a similar delivery technique reported in a previous study [38].

The complex trajectories employed in OXRAY involve numerous manipulation points, which may potentially reduce dosimetric robustness. At these manipulation points, variations in gantry or ring rotation speed are observed, and dose rate adjustments are performed as an alternative to beam on/off switching. Consequently, the accumulated MU at these points slightly exceeds the planned MU. However, a previous study demonstrated that such deviations in accumulated MU have negligible effects on the actual delivered dose [39]. Therefore, the dosimetric robustness of BROAD-RT, even with the use of complex trajectories, can be maintained, ensuring that the enhanced dose distribution achieved by BROAD-RT can be safely implemented in clinical practice.

Our study had several limitations. First, the investigation of trajectory in BROAD-RT was insufficient in our study. We adjusted the trajectories of BROAD-RT to reduce dose variations due to shoulder movement. However, the non-coplanar dynamic trajectory VMAT has the potential to minimize overlapping radiation fields between targets and OARs [13]. Thus, creating an optimal BROAD-RT trajectory for each patient may help achieve further improvement in dose distribution, plan complexity, and delivery time. Second, it is unclear whether BROAD-RT is feasible for patients with head and neck cancers because we did not actually treat patients using OXRAY. To overcome these limitations, we plan to investigate the optimal non-coplanar dynamic trajectory for each patient and conduct a prospective trial to evaluate the feasibility of BROAD-RT for head and neck cancers.

In conclusion, BROAD-RT delivered by OXRAY passed the integration test, and it demonstrated the potential benefit in improving the dose distribution compared to that with COVMAT for patients with nasopharyngeal carcinoma. A prospective trial is required to evaluate the feasibility of BROAD-RT for head and neck cancers, including nasopharyngeal carcinoma.

CRediT authorship contribution statement

Shinya Hiraoka: Writing – original draft, Visualization, Software, Resources, Methodology, Investigation, Formal analysis, Data curation, Conceptualization. **Hideaki Hirashima:** Writing – original draft, Validation, Software, Resources, Methodology, Investigation, Formal analysis, Data curation. **Mitsuhiro Nakamura:** Writing – review & editing, Resources, Methodology, Investigation. **Fumiya Tanaka:** Writing – review & editing, Software, Resources, Methodology, Investigation. **Hiroki Adachi:** Writing – review & editing, Software, Resources,

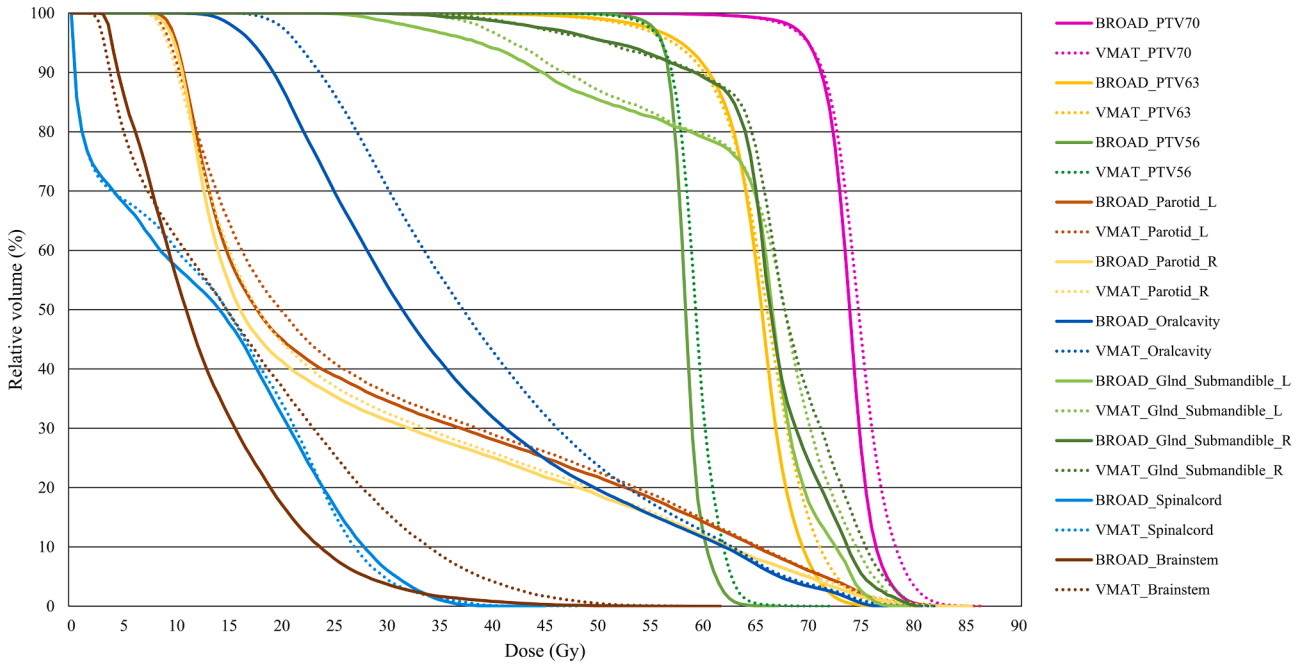

Fig. 3. Representative averaged dose-volume histogram comparison of BROAD-RT and coplanar VMAT for 15 patients. BROAD-RT significantly improved HI of PTV70/63/56 compared with COVMAT. Additionally, BROAD-RT enabled a significant dose reduction compared with COVMAT in $D_{0.03\ cc}$ for the brainstem, D_{mean} for the left submandibular gland, D_{mean} for the right submandibular gland, D_{mean} for the oral cavity, D_{mean} for the left parotid gland, and D_{mean} for the right parotid gland. Abbreviations: BROAD, biaxially rotational dynamic-radiation therapy; VMAT, volumetric arc therapy; PTV, planning target volume; Parotid_L, left parotid gland; Parotid_R, right parotid gland; Glnd_Submandible_L, left submandibular gland; Glnd_Submandible_R, right submandibular gland.

Methodology, Investigation. **Yuka Ono:** Writing – review & editing, Validation, Project administration. **Tomohiro Ono:** Writing – review & editing, Software, Resources. **Ryota Nakashima:** Writing – review & editing, Resources. **Aya Nakajima:** Writing – review & editing, Resources. **Takashi Mizowaki:** Writing – review & editing, Supervision, Project administration, Methodology, Funding acquisition, Conceptualization.

Funding

This study was supported by the Japan Agency for Medical Research and Development (AMED) (JP24ck0106924) and collaborative research agreements with Hitachi High-Tech Corporation.

Declaration of competing interest

The authors declare the following financial interests/personal relationships which may be considered as potential competing interests: Takashi Mizowaki has received research grants and a scholarship donation from Hitachi High-Tech Corp. Mitsuhiro Nakamura has received a scholarship donation from Hitachi High-Tech Corp. The other co-authors are participating in collaborative research with Hitachi High-Tech Corp.

Acknowledgements

We thank Kyoto University Open Innovation Institute for their excellent technical assistance and Editage (www.editage.com) for English language editing.

Appendix A. Supplementary data

Supplementary data to this article can be found online at https://doi.org/10.1016/j.radonc.2025.110879.

Data availability

The data are not publicly available due to privacy or ethical restrictions.

References

[1] Chen YP, Chan ATC, Le QT, Blanchard P, Sun Y, Ma J. Nasopharyngeal carcinoma. *Lancet* 2019;394:64–80. https://doi.org/10.1016/s0140-6736(19)30956-0.
[2] Bossi P, Chan AT, Even C, Machiels JP. ESMO-EURACAN clinical practice guideline update for nasopharyngeal carcinoma: adjuvant therapy and first-line treatment of recurrent/metastatic disease. *Ann Oncol* 2023;34:247–50. https://doi.org/10.1016/j.annonc.2022.11.011.
[3] You R, Liu YP, Huang PY, et al. Efficacy and safety of locoregional radiotherapy with chemotherapy vs chemotherapy alone in de novo metastatic nasopharyngeal carcinoma: A multicenter phase 3 randomized clinical trial. *J Am Med Associat Oncol* 2020;6:1345–52. https://doi.org/10.1001/jamaoncol.2020.1808.
[4] Lee AW, Ng WT, Pan JJ, et al. International guideline for the delineation of the clinical target volumes (CTV) for nasopharyngeal carcinoma. *Radiother Oncol* 2018;126:25–36. https://doi.org/10.1016/j.radonc.2017.10.032.
[5] Mizowaki T, Okajima K, Nagata Y, et al. Concurrent chemotherapy and radiotherapy with low-dose Cisplatin for nasopharyngeal carcinoma. *Am J Clin Oncol* 2003;26:155–8. https://doi.org/10.1097/00000421-200304000-00011.
[6] Du T, Xiao J, Qiu Z, Wu K. The effectiveness of intensity-modulated radiation therapy versus 2D-RT for the treatment of nasopharyngeal carcinoma: A systematic review and meta-analysis. *PLoS One* 2019;14:e0219611. https://doi.org/10.1371/journal.pone.0219611.
[7] Hiraoka S, Yoshimura M, Nakajima A, Nakashima R, Mizowaki T. Long-term outcomes of stimulated salivary flow and xerostomia after definitive intensity-modulated radiation therapy for patients with head and neck cancer. *J Radiat Res* 2024;65:71–7. https://doi.org/10.1093/jrr/rrad087.
[8] Smyth G, Evans PM, Bamber JC, Bedford JL. Recent developments in non-coplanar radiotherapy. *Br J Radiol* 2019;92:20180908. https://doi.org/10.1259/bjr.20180908.
[9] Bertholet J, Mackeprang PH, Loebner HA, et al. Orangs-at-risk dose and normal tissue complication probability with dynamic trajectory radiotherapy (DTRT) for head and neck cancer. *Radiother Oncol* 2024;195:110347. https://doi.org/10.1016/j.radonc.2024.110237.
[10] Dunlop A, Welsh L, McQuaid D, et al. Brain-sparing methods for IMRT of head and neck cancer. *PLoS One* 2015;10:e0120141. https://doi.org/10.1371/journal.pone.0120141.
[11] Leitao J, Bijman R, Wahab Sharfo A, et al. Automated multi-criterial planning with beam angle optimization to establish non-coplanar VMAT class solutions for

nasopharyngeal carcinoma. *Phys Med* 2022;101:20–7. https://doi.org/10.1016/j.ejmp.2022.06.017.
[12] Gayen S, Kombathula SH, Manna S, Varshney S, Pareek P. Dosimetric comparison of coplanar and non-coplanar volumetric-modulated arc therapy in head and neck cancer treated with radiotherapy. *Radiat Oncol J* 2020;38:138–47. https://doi.org/10.3857/roj.2020.00143.
[13] Fix MK, Frei D, Volken W, et al. Part 1: Optimization and evaluation of dynamic trajectory radiotherapy. *Med Phys* 2018;45:4201–12. https://doi.org/10.1002/mp.13086.
[14] Kamino Y, Takayama K, Kokubo M, et al. Development of a four-dimensional image-guided radiotherapy system with a gimbaled X-ray head. *Int J Radiat Oncol Biol Phys* 2006;66:271–8. https://doi.org/10.1016/j.ijrobp.2006.04.044.
[15] Mizowaki T, Takayama K, Nagano K, et al. Feasibility evaluation of a new irradiation technique: three-dimensional unicursal irradiation with the Vero4DRT (MHI-TM2000). *J Radiat Res* 2013;54:330–6. https://doi.org/10.1093/jrr/rrs076.
[16] Uto M, Mizowaki T, Ogura K, et al. Volumetric modulated Dynamic WaveArc therapy reduces the dose to the hippocampus in patients with pituitary adenomas and craniopharyngiomas. *Pract Radiat Oncol* 2017;7:382–7. https://doi.org/10.1016/j.prro.2017.04.004.
[17] Burghelea M, Verellen D, Poels K, et al. Initial characterization, dosimetric benchmark and performance validation of Dynamic Wave Arc. *Radiat Oncol* 2016;11:63. https://doi.org/10.1186/s13014-016-0633-7.
[18] Ono Y, Yoshimura M, Hirata K, et al. Dosimetric advantages afforded by a new irradiation technique, Dynamic WaveArc, used for accelerated partial breast irradiation. *Phys Med* 2018;48:103–10. https://doi.org/10.1016/j.ejmp.2018.03.015.
[19] Burghelea M, Verellen D, Dhont J, et al. Treating patients with Dynamic Wave Arc: First clinical experience. *Radiother Oncol* 2017;122:347–51. https://doi.org/10.1016/j.radonc.2017.01.006.
[20] Ono T, Miyabe Y, Yamada M, et al. Development of an expanded-field irradiation technique using a gimbaled x-ray head. *Med Phys* 2014;41:101706. https://doi.org/10.1118/1.4895016.
[21] Ono T, Miyabe Y, Yokota K, et al. Development of a gimbal-swing irradiation technique for uniform expanded-field, wedged-beam, and intensity-modulated radiation therapy. *Biomed Phys Eng Express* 2016;2. https://doi.org/10.1088/2057-1976/2/6/065007.
[22] Ono T, Miyabe Y, Takahashi K, et al. Geometric and dosimetric accuracy of dynamic tumor tracking during volumetric-modulated arc therapy using a gimbal mounted linac. *Radiother Oncol* 2018;129:166–72. https://doi.org/10.1016/j.radonc.2017.10.034.
[23] Hiraoka M, Mizowaki T, Matsuo Y, et al. The gimbaled-head radiotherapy system: Rise and downfall of a dedicated system for dynamic tumor tracking with real-time monitoring and dynamic WaveArc. *Radiother Oncol* 2020;153:311–8. https://doi.org/10.1016/j.radonc.2020.07.002.
[24] Stronger and more flexible X-ray radiotherapy. Hitachi Ltd. *Nature Portfolio*. 2024. https://www.nature.com/articles/d42473-023-00445-6.
[25] Brierley JD, Gospodarowicz MK, Wittekind C. TNM classification of malignant tumours. John Wiley & Sons; 2017.
[26] Brouwer CL, Steenbakkers RJ, Bourhis J, et al. CT-based delineation of organs at risk in the head and neck region: DAHANCA, EORTC, GORTEC, HKNPCSG, NCIC CTG, NCRI, NRG Oncology and TROG consensus guidelines. *Radiother Oncol* 2015;117:83–90. https://doi.org/10.1016/j.radonc.2015.07.041.
[27] Tachibana H, Motegi K, Moriya S, et al. Impact of shoulder deformation on volumetric modulated arc therapy doses for head and neck cancer. *Phys Med* 2018;53:118–28. https://doi.org/10.1016/j.ejmp.2018.08.015.
[28] Wu Q, Mohan R, Morris M, Lauve A, Schmidt-Ullrich R. Simultaneous integrated boost intensity-modulated radiotherapy for locally advanced head-and-neck squamous cell carcinomas. I: dosimetric results. *Int J Radiat Oncol Biol Phys* 2003;56. https://doi.org/10.1016/s0360-3016(02)04617-5. pp. 573–85.3.
[29] Paddick I. A simple scoring ratio to index the conformity of radiosurgical treatment plans. J Neurosurg 2000;93:219–22. https://doi.org/10.3171/jns.2000.93.supplement.
[30] Hansen CR, Crijns W, Hussein M, et al. Radiotherapy Treatment plannINg study Guidelines (RATING): A framework for setting up and reporting on scientific treatment planning studies. *Radiother Oncol* 2020;153:67–78. https://doi.org/10.1016/j.radonc.2020.09.033.
[31] McNiven AL, Sharpe MB, Purdie TG. A new metric for assessing IMRT modulation complexity and plan deliverability. *Med Phys* 2010;37:505–15. https://doi.org/10.1118/1.3276775.
[32] Masi L, Doro R, Favuzza V, et al. Impact of plan parameters on the dosimetric accuracy of volumetric modulated arc therapy. *Med Phys* 2013;40:071718. https://doi.org/10.1118/1.4810969.
[33] Miften M, Olch A, Mihailidis D, et al. Tolerance limits and methodologies for IMRT measurement-based verification QA: Recommendations of AAPM Task Group No. 218. *Med Phys*. 2018;45(4):e53-e83. DOI: 10.1002/mp.12810.
[34] Lincoln JD, Macdonald RL, Syme A, Thomas CG. Static couch non-coplanar arc selection optimization for lung SBRT treatment planning. *Phys Med Biol* 2023;68:155011. https://doi.org/10.1088/1361-6560/ace23f.
[35] Bertholet J, Mackeprang PH, Mueller S, et al. Organ-at-risk sparing with dynamic trajectory radiotherapy for head and neck cancer: comparison with volumetric arc therapy on a publicly available library of cases. *Radiat Oncol* 2022;17:122. https://doi.org/10.1186/s13014-022-02092-5.
[36] Hadj Henni A, Gensanne D, Roge M, et al. Evaluation of inter- and intra-fraction 6d motion for stereotactic body radiation therapy of spinal metastases: Influence of treatment time. *Radiat Oncol* 2021;16:168. https://doi.org/10.1186/s13014-021-01892-5.
[37] Subramanian VS, Subramani V, Chilukuri S, et al. Multi-isocentric 4pi volumetric-modulated arc therapy approach for head and neck cancer. *J Appl Clin Med Phys* 2017;18:293–300. https://doi.org/10.1002/acm2.12164.
[38] Hirashima H, Nakamura M, Miyabe Y, et al. Geometric and dosimetric quality assurance using logfiles and a 3D helical diode detector for Dynamic WaveArc. *Phys Med* 2017;43:107–13. https://doi.org/10.1016/j.ejmp.2017.10.023.
[39] Sato S, Miyabe Y, Takahashi K, et al. Commissioning and quality assurance of Dynamic WaveArc irradiation. *J Appl Clin Med Phys* 2015;16:73–86. https://doi.org/10.1120/jacmp.v16i2.5080.